TWMS J. App. Eng. Math. V.10 , No.1, 2020, pp. 181-189

BACKSCATTERING FROM SOFT-HARD TRIANGULAR CYLINDER: PRIMARY PTD APPROXIMATION

F. HACIVELIOGLU[1], §

Abstract. High-frequency diffraction from isosceles triangular cylinders with two faces soft and one face hard is investigated for backscattering case and novel first-order physical theory of diffraction asymptotics are derived. Only primary edge waves are taken into account. It is shown that, by changing the apex angle of the cylinder, PTD results of the soft-hard triangular cylinder agree-well with those of the PTD results of Soft-Hard Strip.

Keywords: asymptotic diffraction theory, backscattering, far zone field, physical theory of diffraction, scattering.

AMS Subject Classification: 78A10, 78A45

1. Introduction

One of the techniques used in the reduction of radar cross section (RCS) of an object is "shaping". A polygonal cylinder is one of few objects used for this purpose. Scattering from the polygonal cylinders has been investigated in many publications by using different numerical and analytical techniques [1]-[7]. Backscattering from a triangular cylinder and hexahedron are studied in [8] by modified equivalent current method. In [9] Physical Optics (PO) and Physical Theory of Diffraction (PTD) solutions are derived for bi-static and monostatic cases at both soft and hard cylinders with triangular cross section. More accurate PTD results, without singularities for any incident and observation directions, are obtained for the above-mentioned problem by Johansen in [10] using the truncated equivalent edge currents. Backscattering by triangular dielectric cylinders is analyzed by the method of analytical regularization [11]. In [12], backscattering from a dielectric cylinder with triangular cross section is investigated in terms of ray-like wave pieces and resonances. Lately, first-order PTD approximation of trilateral cylinders with combinations of soft and hard faces is investigated in [13], and the results are confirmed by the method of moments. The aim of this paper is to investigate the primary PTD approximation for backscattering case, and introduce the advantages and shortcomings of the first-order approximation. The geometry of the problem is isosceles triangular cylinder with two faces soft and one hard. In the primary PTD approximation, the far field scattered by

[1] Gebze Technical University, Mathematical Department, Gebze, Kocaeli, Turkey.
e-mail: f.dagidir@gtu.edu.tr; ferayhvo@gmail.com; ORCID: https://orcid.org/0000-0003-0394-3736.

§ Manuscript received: June 07, 2018; accepted: December 30, 2018.
TWMS Journal of Applied and Engineering Mathematics, Vol.10, No.1;

a triangular cylinder is a linear combination of the edge waves generated by the edges on the triangular cylinder. Higher-order asymptotic fields are much weaker in magnitude than the first-order asymptotic fields. The orders of the doubly diffracted fields along the soft and hard faces are $(kl)^{-3/2}$ and $(kl)^{-1/2}$ respectively [9]-[14]. Therefore, in this paper, only first-order asymptotic fields, which are of practical interest for the engineering purpose, are evaluated. The results when the apex angle goes to π are compared with the first order PTD results of the soft-hard strip problem [15], which is validated by MoM in [16]. The paper is organized as follows: In Section II, for the sake of completeness, exact and asymptotic solutions of the canonical wedge problems are summarized for the cases both faces soft and hard, and one face soft the other one hard. In Section III, geometry of the problem is introduced and related directivity functions of the edge waves are given for the backscattering case. PO and PTD fields are derived in Section IV. Some graphical results of radar cross section are presented in Section V. Concluding remarks are given in Section VI.

2. Canonical Wedge Problem

Diffraction at a wedge with infinite planar faces is a canonical problem in high-frequency asymptotic techniques. Exact solution of this problem in particular case of half-plane was first given by Sommerfeld in 1896 [17]. In 1902, Macdonald obtained general solutions for (i) a two dimensional (2D) wedge with arbitrary angle under the plane wave and line source illuminations, (ii) a 3D wedge with arbitrary angle under a point source illumination [18]. Later, Sommerfeld developed simple asymptotic expressions for edge-diffracted waves [19].

Incident plane wave given by

$$u^{inc} = e^{-ikr\cos(\phi-\phi_0)} \tag{1}$$

illuminates the wedge presented in Figure 1.

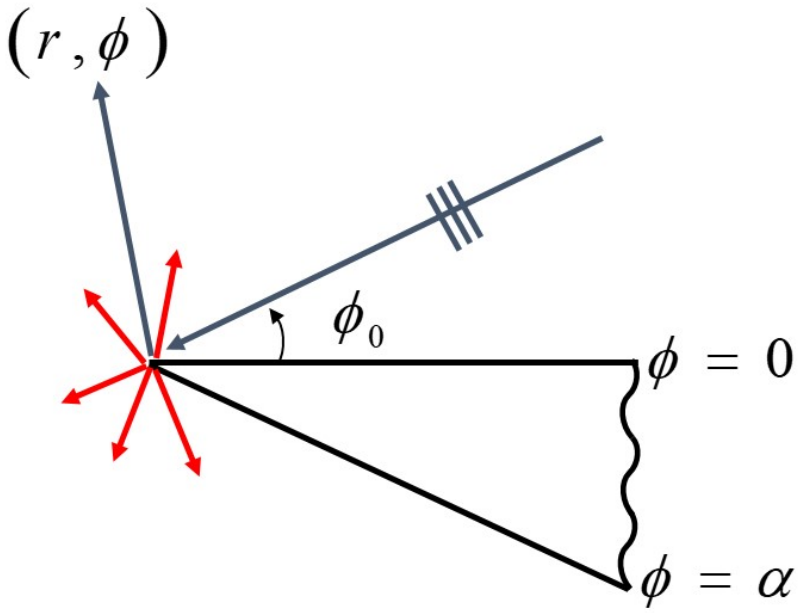

Figure 1. Geometry of the wedge problem.

Field outside the wedge ($0 < \phi < \alpha$) satisfies the homogeneous Helmholtz equation

$$\nabla^2 u + k^2 u = 0 \tag{2}$$

where ∇^2 is the Laplacian operator, u is the scattered field and $k = 2\pi/\lambda$ is the wave number, λ the wavelenght. The time dependence is in the form of $\exp(-i\omega t)$.

Here, four cases are under consideration:

1) Upper and lower faces of the wedge are soft ($u = 0$ if $\phi = 0, \alpha$)
2) Upper and lower faces of the wedge are hard ($\partial u/\partial n = 0$ if $\phi = 0, \alpha$)
3) Upper face is soft ($u = 0$ if $\phi = 0$) and lower face is hard ($\partial u/\partial n = 0$ if $\phi = \alpha$)
4) Upper face is hard ($\partial u/\partial n = 0$ if $\phi = 0$) and lower face is soft ($u = 0$ if $\phi = \alpha$)

Since the case 3 and 4 admit double electromagnetic interpretation, acoustic terms are used for all cases avoiding possible confusing.

Helmholtz equation is solved under i) the boundary conditions given above, ii) radiation condition

$$\lim_{r\to\infty} \sqrt{r}\left(\frac{\partial u}{\partial r} - iku\right) = 0 \tag{3}$$

and iii) edge condition

$$u = O\left[(kr)^p\right] \tag{4}$$

where $p = \pi/\alpha$ for cases 1, 2 and $p = \pi/2\alpha$ for cases 3, 4.

It is known that, the solution of the boundary value problem (2)-(4) exists and is unique. The exact solution is as follows:

$$u^{exact} = u(kr, \phi - \phi_0) \mp u(kr, \phi + \phi_0) \tag{5}$$

upper sign in (5) refers to the wedge in cases 1, 3 and the lower to the cases 2, 4. Here,

$$u(kr, \psi) = \frac{2\pi}{\alpha} \sum_{l=0}^{\infty} e^{-i\pi\nu_l/2} J_{\nu_l}(kr) \cos\nu_l\psi \tag{6}$$

with $\nu_l = l\pi/\alpha$ for the cases 1, 2 and $\nu_l = (2l+1)\pi/\alpha$ for the cases 3, 4.

The series in (6) is converted to the Sommerfeld-type integral for an asymptotic evaluation. As a result, diffracted field is found as

$$u^{dif} = f(\phi, \phi_0) \frac{e^{i(kr+\pi/4)}}{\sqrt{2\pi kr}} \tag{7}$$

Here, function f is directivity pattern of the edge wave.

The details of the solutions can be found in [9] for the cases 1, 2 and in [20] for the case 3. Asymptotic solution for the case 4 can be obtained easily following similar processes in [20].

3. Backscattering from soft-hard triangular cylinder

The geometry of the two dimensional triangular cylinder is depicted in Figure 2.

The points 1, 2 and 3 are the edges whose Cartesian coordinates are $(0, 0)$, (h, a), and $(h, -a)$ where $h = l\cos\gamma$ and $h = l\sin\gamma$. Faces 1-2 and 1-3 are imposed to soft boundary condition and face 2-3 is imposed hard boundary condition.

The incident wave is given by

$$u^{inc} = e^{-ik(x\cos\varphi_0 + y\sin\varphi_0)} \quad \text{with} \quad 0 \le \varphi_0 \le 2\pi \tag{8}$$

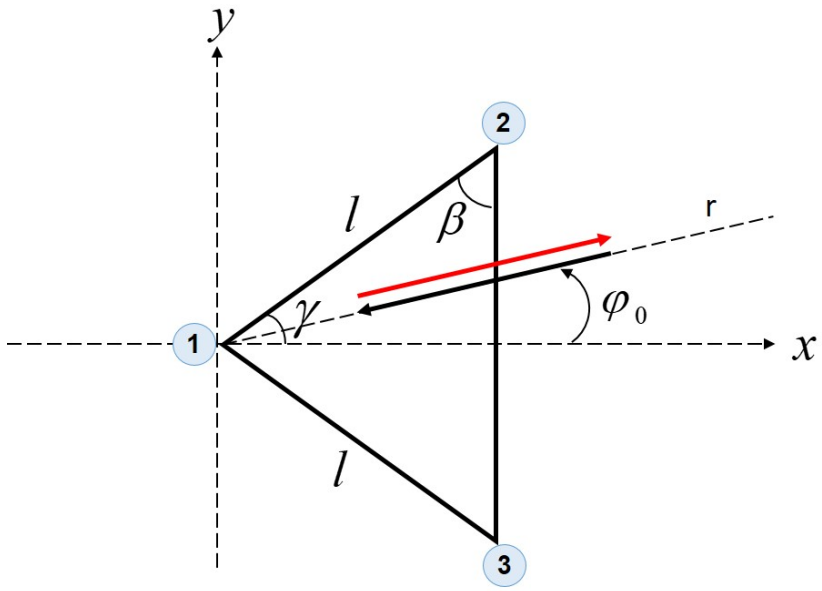

FIGURE 2. Cross-section of the isosceles triangular cylinder.

Scattered field is evaluated in the direction $\varphi = \varphi_0$ in the far-zone ($r \gg kl^2$). Local polar coordinates $(r_{1,2,3}, \phi_{1,2,3})$ are used for the edge waves where $\phi_{1,2,3}$ are measured from the illuminated side of the cylinder (Figure 3).

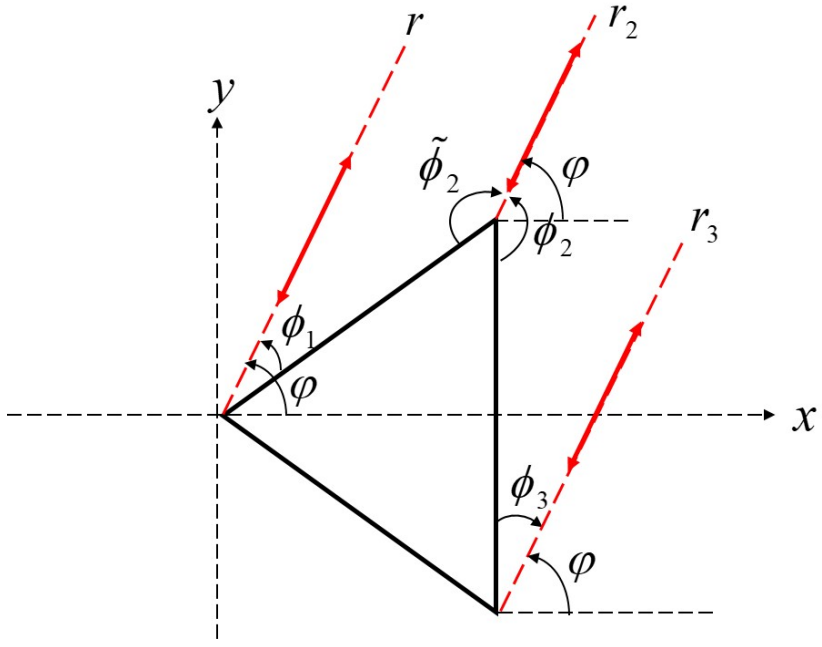

FIGURE 3. Local coordinates for edge waves.

Diffracted fields (PO and PTD) from all edges in the far zone are given by (7). Here the function $f(\phi)$ is $f_s^{(0)}$ and $f_h^{(0)}$ for the PO field in case upper face (illuminated face)

of the wedge is soft and hard respectively and f_s, f_h, f_{sh} and f_{hs} for the PTD field in case totally soft, totally hard, upper face is soft, lower face is hard and upper face is hard, lower face is soft wedge respectively:

$$f_s^{(0)}(\phi) = \frac{1}{2}\tan\phi \text{ and } f_h^{(0)}(\phi) = -f_s^{(0)} \tag{9}$$

which are the result of (3.59) in [9],

$$\left.\begin{matrix} f_s(\phi) \\ f_h(\phi) \end{matrix}\right\} = \frac{1}{n}\sin\left(\frac{\pi}{n}\right)\left(\frac{1}{\cos(\pi/n)-1} \mp \frac{1}{\cos(\pi/n)-\cos(2\phi/n)}\right) \tag{10}$$

which are the result of (2.62) and (2.64) in [9].

$$\left.\begin{matrix} f_{sh}(\phi) \\ f_{hs}(\phi) \end{matrix}\right\} = \frac{2}{n}\sin\left(\frac{\pi}{2n}\right)\left(\frac{1}{\cos(\pi/n)-1} \mp \frac{\cos(\phi/n)}{\cos(\pi/n)-\cos(2\phi/n)}\right) \tag{11}$$

where f_{sh} follows from (19) of [20]. f_{sh} can be derived easily by using the similar process in [20].

Here $n = \alpha/\pi$ and $0 \le \phi \le \alpha$ (Figure 1).

4. PO and PTD fields

PO and PTD fields for the soft-hard triangular cylinder are calculated as the sum of the three edge waves

$$u^{dif} = \sum_{m=1}^{3} \varepsilon_m u_0(m) f(\phi_m) \frac{e^{i(kr_m+\pi/4)}}{\sqrt{2\pi k r_m}} \tag{12}$$

Here $\varepsilon_m = 1$ when the edge m is seen, otherwise $\varepsilon_m = 1$, $m = 1,2,3$. $u_0(1) = u_0$, $u_0(2) = u_0 e^{ik(h\cos\varphi + a\sin\varphi)}$ and $u_0(3) = u_0 e^{ik(h\cos\varphi - a\sin\varphi)}$. u^{dif} represents PO or PTD field depending on the function f which has the forms $f_s^{(0)}$ and $f_h^{(0)}$ for the PO field and f_s, f_h, f_{sh} and f_{hs} for the PTD field.

For the far field ($r \gg kl^2$), if we take $r_1 = r$, then $r_2 = r - h\cos\varphi - a\sin\varphi$, $r_3 = r - h\cos\varphi + a\sin\varphi$ where $r_{1,2,3}$ are measured from the edges 1, 2, 3 and we have

$$u^{sc} = u_0 \sum_{m=1}^{3} \Phi(\varphi) \frac{e^{i(kr+\pi/4)}}{\sqrt{2\pi kr}} \tag{13}$$

where $\Phi(\varphi) = \varepsilon_m f(m) e^{i\psi_m}$ with $f(m) \equiv f(\phi_m)$, $\psi_1 = 0$, $\psi_2 = -2kl\cos(\gamma - \varphi)$ and $\psi_3 = -2kl\cos(\gamma + \varphi)$.

In the interval $0 \le \varphi \le \gamma$ diffracted fields consist of the waves from edges 2 and 3. In this interval directivity pattern of PTD and PO fields are

$$\Phi^{PTD} = f_{hs}(2) e^{i\psi_2} + f_{hs}(3) e^{i\psi_3} \tag{14}$$

$$\Phi^{PO} = -i\cot\varphi \sin(2ka\sin\varphi) e^{-i2kh\cos\varphi} \tag{15}$$

where

$$f_{hs}(2) = \frac{2}{n_2}\sin\left(\frac{\pi}{n_2}\right)\left(\frac{1}{\cos\frac{\pi}{n_2}-1} + \frac{\cos\frac{\pi+2\varphi}{2n_2}}{\cos\frac{\pi}{n_2}-\cos\frac{\pi+2\varphi}{n_2}}\right) \tag{16}$$

$$f_{hs}(3) = \frac{2}{n_2}\sin\left(\frac{\pi}{n_2}\right)\left(\frac{1}{\cos\frac{\pi}{n_2}-1} + \frac{\cos\frac{\pi-2\varphi}{2n_2}}{\cos\frac{\pi}{n_2}-\cos\frac{\pi-2\varphi}{n_2}}\right) \tag{17}$$

For the direction $\varphi = 0$

$$\Phi^{PTD}(0) = \left(-i2ka - \frac{1}{n_2 \sin\frac{\pi}{n_2}} + \frac{\frac{4}{n_2}\sin\frac{\pi}{2n_2}}{\cos\frac{\pi}{n_2} - 1} \right) e^{-i2kh} \tag{18}$$

$$\Phi^{PO}(0) = -i2kl \sin\gamma e^{-i2kl\cos\gamma} \tag{19}$$

In the interval $\gamma \leq \varphi \leq \pi/2$ an additional wave coming from edge 1 appears and

$$\Phi^{PTD} = f_s(1) + f_{hs}(2)\, e^{i\psi_2} + f_{hs}(3)\, e^{i\psi_3} \tag{20}$$

$$\Phi^{PO} = -i\tan(\gamma-\varphi)\sin(2kl\cos(\gamma-\varphi))\, e^{i\psi_2/2} - i\cot\varphi \sin(2ka\sin\varphi)\, e^{-i2kh\cos\varphi} \tag{21}$$

where

$$f_s(1) = \frac{1}{n_1}\sin\left(\frac{\pi}{n_1}\right)\left(\frac{1}{\cos\frac{\pi}{n_1} - 1} - \frac{1}{\cos\frac{\pi}{n_1} - \cos\frac{2\varphi - 2\gamma}{n_1}}\right) \tag{22}$$

$f_{hs}(2)$ and $f_{hs}(3)$ are same as (16), (17) respectively.

In the interval $\pi/2 \leq \varphi \leq \pi - \gamma$ edge 3 is not seen and

$$\Phi^{PTD} = f_s(1) + f_{sh}(2)\, e^{i\psi_2} \tag{23}$$

$$\Phi^{PO} = -i\tan(\gamma-\varphi)\sin(kl\cos(\gamma-\varphi))\, e^{i\psi_2/2} \tag{24}$$

In the interval $\pi - \gamma \leq \varphi \leq \pi$ scattered field is generated by all three edges again:

$$\Phi^{PTD} = f_s(1) + f_{sh}(2)\, e^{i\psi_2} + f_{sh}(3)\, e^{i\psi_3} \tag{25}$$

$$\Phi^{PO} = -i\tan(\gamma-\varphi)\sin(kl\cos(\gamma-\varphi))\, e^{i\psi_2/2} - i\tan(\gamma+\varphi)\sin(kl\cos(\gamma+\varphi))\, e^{i\psi_3/2} \tag{26}$$

where

$$f_{sh}(3) = \frac{2}{n_2}\sin\left(\frac{\pi}{n_2}\right)\left(\frac{1}{\cos\frac{\pi}{n_2} - 1} - \frac{\cos\frac{\pi-\gamma-\varphi}{2n_2}}{\cos\frac{\pi}{n_2} - \cos\frac{2\pi - 2\gamma - 2\varphi}{n_2}}\right) \tag{27}$$

$f_{sh}(2)$ in (25) coincides with $f_{hs}(2)$ the function in (16).

5. Numerical results

Numerical calculations are carried out for the normalized scattering cross section which is defined as [9]

$$\sigma_{norm} = 10\log\left|\frac{\Phi(\varphi)}{kl}\right|^2 \tag{28}$$

Calculations are performed only in the interval $0 \leq \varphi \leq \pi$ due to the symmetric scattering with respect to $x-$axis.

In Figure 4, the curves PTD-Soft and PTD-Hard represent the backscattering field from totally soft and totally hard cylinders with $\gamma = \pi/6$, and were calculated according to Section 5.2.4 in [9]. It is seen that the discontinuities in the directions $\phi = \gamma$ and $\phi = \pi - \gamma$ in the case of totally hard cylinder are removed in the soft-hard cylinder. This is due to the doubly diffracted fields. Doubly diffracted field generated by the single diffracted field along the soft face is of the order of $(kl)^{-3/2}$. This is in the order of $(kl)^{-1/2}$ in the case of hard face. That is why the discontinuity in the direction $\phi = \pi/2$ is still preserved. In the direction $\phi = \pi/2$, backscattering field has double diffracted field along the hard face from the edge 3.

In Figure 5, the curves PO-Soft and PO-Hard represent the backscattering field from totally soft and totally hard cylinders and were calculated according to Section 5.2.2 in [9]. The PO field in the region $40^0 < \phi < 80^0$ for the soft-hard triangular cylinder differs from

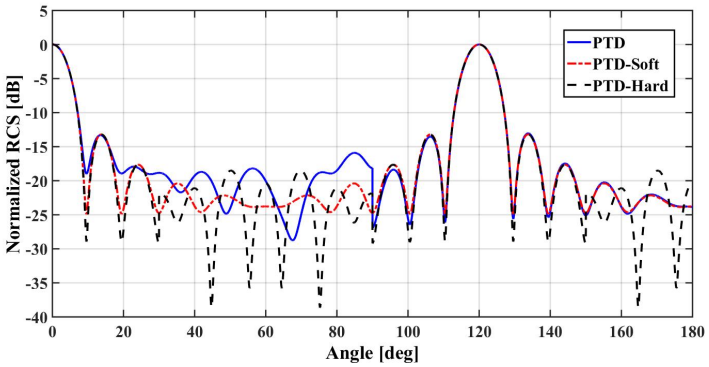

FIGURE 4. Comparison of PTD fields from Soft-Hard cylinder, totally soft and totally hard cylinder ($\gamma = 30^0$, $kl = 6\pi$).

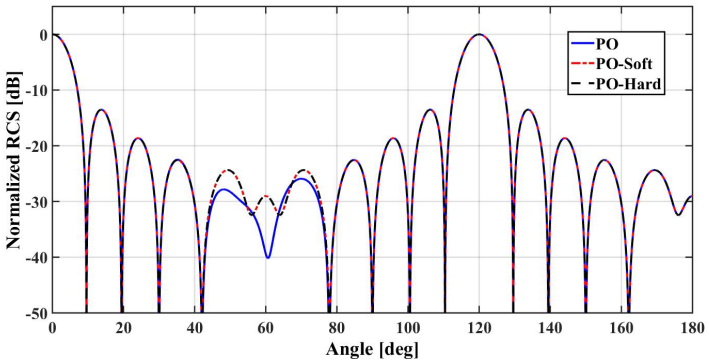

FIGURE 5. Comparison of PO fields from Soft-Hard cylinder, totally soft and totally hard cylinder ($\gamma = 30^0$, $kl = 6\pi$).

the PO fields for the totally soft and totally hard cylinders. That is why the backscattering PO field consists of the sum of the edge waves from the all edges. In this region, edges 1, 2, and 3 are illuminated from the soft, soft and hard, and hard face, respectively. Although the backscattering field in the region $150^0 < \phi < 180^0$ consists of the edge waves from the all edges, it is same as the totally soft or totally hard cylinder. Because, in this region, as in the case of totally soft cylinder, all edges are illuminated from the soft faces. Note that, directivity pattern of totally soft and totally hard cylinders differ only in sign [9].

Figure 6 demonstrates the PTD, PO and Fringe fields for right-angle triangular cylinder where $\gamma = \pi/4$. Fringe field is calculated subtracting PO field from PTD field:

$$u^{fringe} = u^{PTD} - u^{PO} \tag{29}$$

Effect of the double diffracted fields is also seen in this figure in the direction $\phi = \pi/2$.

Figure 7 compares the backscattering field from soft-hard triangular cylinder and soft-hard strip in [15]. When the apex angle of the triangular cylinder approaches π, results from the soft-hard triangular cylinder get close to the results from soft-hard strip in [15] which is validated by MoM in [16].

In all figures $l = 3\lambda$ is taken.

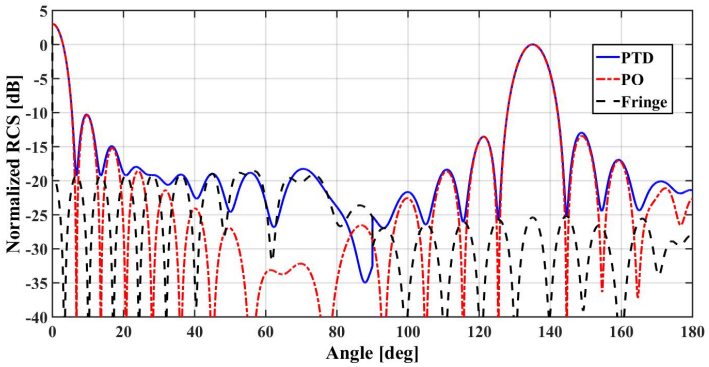

FIGURE 6. Backscattering at the right-angle triangular cylinder ($\gamma = 45^0$, $kl = 6\pi$).

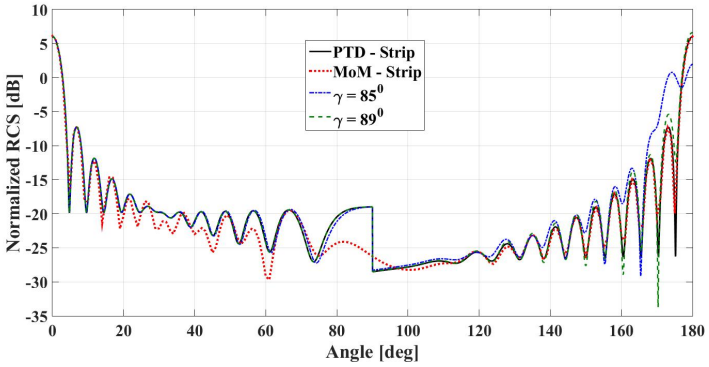

FIGURE 7. Comparison of backscattering fields from Soft-Hard cylinder and Soft-Hard strip ($kl = 6\pi$).

6. CONCLUSION

The novel first-order asymptotics, consist of first-order edge waves scattered by three canonical wedges, for the backscattering from soft-hard isosceles triangular cylinder have been derived using physical theory of diffraction. Numerical calculations of these solutions given by trigonometric functions are very easy. Normalized scattering cross section in dB scale is calculated for the soft-hard equilateral and right-angle triangular cylinders and are compared with the results from totally soft and hard cylinders. It is seen that, discontinuities due to doubly diffracted fields in the backscattering field for the totally hard cylinder are removed in the backscattering field for the soft-hard cylinder, except in the direction $\phi = \pi/2$. The solutions when the half of the apex angle of the triangular cylinder approaches π, results from the soft-hard triangular cylinder and the results from soft-hard strip also agree very well with MoM solutions.

Acknowledgement. The author would like to thank to the authors of the reference [16] for the MoM codes in Figure 7.

REFERENCES

[1] Morse, B. J., (1964), Diffraction by polygonal cylinders. J Math Phys, 5, 2, pp. 199-214. Erdelyi, A., (1956), Asymptotic expansions, Dover publications, New York.

[2] Rusch, W. V. T., (1978), Forward scattering from cylinders of triangular cross section. IEEE T Antenn Propag, 26, 6, pp. 849-850.
[3] Michaeli A., (1987), A uniform GTD solution for the far-field scattering by polygonal cylinders and strips. IEEE T Antenn Propag, 35, 8, pp. 983-986.
[4] Tiberio, R., Manara, G., Pelosi, G., Kouyoumjian, R. G., (1989), High-frequency electromagnetic scattering of plane waves from double wedges. IEEE T Antenn Propag, 37, 9, pp. 1172-1180.
[5] Veliev, E.I., Veremey, V.V., (1993), Numerical analytical approach for the solution to the wave scattering by polygonal cylinders and flat strip structures. In: Hashimoto, M., Idemen, M., Tretyakov, O.A., editors. Analytical and Numerical Methods in Electromagnetic Wave Theory. Tokyo Science House.
[6] Wu, J., Mostafavi, M., (1993), Higher order UTD analysis of a conducting triangular cylinder excited by a magnetic line source. IEEE T Magn, 29, 2, pp. 1650-1652.
[7] Lucido, M., Panariello, G., Schettino, F., (2006), Analysis of the electromagnetic scattering by perfectly conducting convex polygonal cylinders. IEEE T Antenn Propag, 54, 4, pp. 1223-1231.
[8] Sunahara, Y., Kaniya, S., Aoki, H., Sato, S., Mano, S., (1986) Backscattering from triangular cylinder and hexahedron. In: Antennas and Propagation Society International Symposium, Philadelphia, USA, IEEE, pp. 49-52.
[9] Ufimtsev, P. Ya., (2014), Fundamentals of the physical theory of diffraction. 2nd ed. Hoboken, USA, John Wiley and Sons, Inc.
[10] Johansen, P. M., (1996), Uniform physical theory of diffraction equivalent edge currents for truncated wedge strips. IEEE T Antenn Propag, 44, pp. 989-995.
[11] Illyashenko, L. N., (2002), Electromagnetic backscattering from a triangular dielectric cylinder. In: IX International conference on mathematical methods in electromagnetic theory, Kiev, Ukraine, IEEE, pp. 592-593.
[12] Sukharevsky, I. O., Nosich A. I., Altintas A., (2015), Manipulation of backscattering from a dielectric cylinder of triangular cross-section using the interplay of GO-like ray effects and resonances. IEEE T Antenn Propag, 63, 5, pp. 2162-2168.
[13] Hacivelioglu, F., Apaydin, G., Sevgi, L., Ufimtsev, P. Ya., (2018), Diffraction at trilateral cylinders with combinations of soft and hard faces: first-order PTD approximation, Electromagnetics, 38, 4, pp. 217-225.
[14] Buyukaksoy, A., Alkumru, A., (1995), Multiple diffraction of plane waves by soft/hard strip. J Eng Math, 29, pp. 105-120.
[15] Hacivelioglu, F., Sevgi, L., Ufimtsev, P. Ya., (2013), Backscattering from a soft-hard strip: primary edge waves approximations. IEEE Antenn Wirel Pr, 12, pp. 249-252.
[16] Apaydin, G., Sevgi, L., (2015), Method of moments modeling of backscattering by a soft-hard strip. IEEE T Antenn Propag, 63, pp. 5822-5826.
[17] Sommerfeld, A., (1896), Mathematische Theorie der diffraction. Math Ann, 47, pp. 317-374.
[18] Macdonald, H.M., (1902), Electric waves. Cambridge, UK: Cambridge University Press.
[19] Sommerfeld, A.,(1935), Theorie der Beugung. In: Frank F. and Mizes R.V., editors. Die Differential und integralgleichungen der mechanik und physik. Braunschweig, Germany, Wieweg and Sohn (American Publications, New York, 1943, 1961).
[20] Ufimtsev, P. Ya., (2013), Diffraction at a wedge with one face electric and the other face magnetic. IEEE Antenn Propag Magazine, 55, 5, pp. 63-73.

Feray Hacivelioglu received B.S. in Mathematical Engineering from Yildiz Technical University, Turkey in 2002, M.S and Ph.D. degrees in Mathematics from Gebze Institute of Technology, Turkey in 2004, 2010 respectively. She studied diffraction from coaxial waveguides with impedance and groove type discontinuities by using the Wiener-Hopf technique in her PhD dissertation. She was a postdoctoral researcher at Electronics and Communications Engineering Department of Dogus University from 2010 to 2011. She studied Physical Optics (PO) and Pyhsical Theorey of Diffraction (PTD), high frequency techniques based on induced currents on the surface of the object. She has been with Gebze Technical University since September 2002. She is an assistant professor in Department of Mathematics in Gebze Technical University. Her research interests are diffraction theory, mixed-boundary value problems (Wiener-Hopf Technique) and high frequency techniques.